

Laser Photoelectron Spectrometry of $\text{Ni}(\text{CO})_n^-$, $n = 1-3$

Amy E. Stevens, C. S. Feigerle, and W. C. Lineberger*

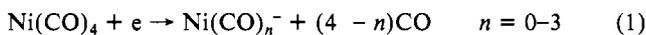
Contribution from the Department of Chemistry, University of Colorado and Joint Institute for Laboratory Astrophysics, University of Colorado and National Bureau of Standards, Boulder, Colorado 80309. Received February 24, 1982

Abstract: Photoelectron spectra of the negative ions $\text{Ni}(\text{CO})_n^-$, $n = 1-3$, obtained with a fixed-frequency argon-ion laser operating at 488 nm are reported. The spectra provide the electron affinities for this series, $\text{EA}[\text{Ni}(\text{CO})] = 0.804 \pm 0.012$ eV, $\text{EA}[\text{Ni}(\text{CO})_2] = 0.643 \pm 0.014$ eV, and $\text{EA}[\text{Ni}(\text{CO})_3] = 1.077 \pm 0.013$ eV. The symmetric C-O vibrational frequencies for the neutral complexes are obtained from the spectra. Metal-carbonyl bond strengths for the neutral carbonyls, $\text{Ni}(\text{CO})_n$, $n = 1-4$, are derived from these and other data. Electronic and geometric structure of ions and neutrals is also discussed.

Introduction

Highly unsaturated transition-metal carbonyl complexes play an important role in processes such as homogeneous catalysis and single-photon¹ and multiphoton² decomposition of organometallics. The monoligated atoms, in particular, are often considered as a model for CO binding to a metal surface.³⁻⁷ We report the laser photoelectron spectra of the nickel carbonyl ions, $\text{Ni}(\text{CO})_n^-$, $n = 1-3$. These data provide insight into the electronic and geometric structure of ion and neutral, yield carbonyl vibrational frequencies for the neutral, and, in conjunction with other data, provide the nickel-carbonyl bond energies for all the $\text{Ni}(\text{CO})_n$, $n = 1-4$.

Several techniques have been utilized to study both the nickel carbonyl ions and neutrals. The ions $\text{Ni}(\text{CO})_n^-$, $n = 0-3$, are all observed in the negative ion mass spectrum of $\text{Ni}(\text{CO})_4$; they are produced by dissociative attachment of an electron to $\text{Ni}(\text{CO})_4$, reaction 1.⁸ The $\text{Ni}(\text{CO})_4^-$ ion is not bound with respect to loss of CO.⁸



The appearance potentials, AP, of the ions in process 1 have been determined by Compton and Stockdale.⁸ These data provide the nickel carbonyl bond dissociation energies for the negative ions, as given by eq 2.

$$D[\text{Ni}(\text{CO})_{n-1}^- - \text{CO}] = \text{AP}[\text{Ni}(\text{CO})_{n-1}^-] - \text{AP}[\text{Ni}(\text{CO})_n^-] \quad (2)$$

The photochemistry of $\text{Ni}(\text{CO})_3^-$ has been studied⁹ using the techniques of ion cyclotron resonance spectroscopy (ICR). This molecule was observed to "photodisappear" when irradiated, with a threshold at about 2.0 eV and a peak at about 2.5 eV photon energy. The photoproduct was not conclusively identified; production of Cl^- with added CCl_4 was observed and is probably an indication of electron detachment occurring, but this could not be quantified. Finally, the $\text{Ni}(\text{CO})_3^-$ ion has been produced by vacuum-UV photolysis of $\text{Ni}(\text{CO})_4$ isolated in an argon matrix, and identified by infrared spectroscopy.^{10,11}

There is also information available on the neutral complexes. The fragments $\text{Ni}(\text{CO})_n$, $n = 1-3$, are produced either by reaction of Ni atoms with CO in an argon matrix,¹² or by vacuum-UV photolysis of $\text{Ni}(\text{CO})_4$ isolated in an argon matrix.^{10,11} They are identified by the C^{16}O and C^{18}O infrared stretching frequencies. $\text{Ni}(\text{CO})_3$,^{7,13-15} and $\text{Ni}(\text{CO})_2$,^{7,13} have been the object of molecular orbital calculations, and several groups have reported calculations on the electronic states of $\text{Ni}(\text{CO})$.³⁻⁷

Experimental Section

The experimental apparatus for laser photoelectron spectroscopy has been described.¹⁶ Briefly, it consists of an electrical discharge ion source from which negative ions are extracted, accelerated to 680 eV and mass-analyzed by a Wien filter. The mass-selected beam is crossed with the 488 nm (2.540 eV) photons of an intracavity CW argon-ion laser. Photodetached electrons ejected perpendicular to the laser and ion beams are energy analyzed in a hemispherical electron monochromator, with resolution approximately 45 meV fwhm.

The absolute, center-of-mass electron kinetic energies, E_X , are determined by using simultaneously produced O^- as a calibrant ion. Applying an energy balance to both O^- and species X yields eq 3, in which $h\nu = 2.540$ eV; $\text{EA}(\text{O}) = 1.465$ eV is the "effective" electron affinity of the

$$E_X = h\nu - \text{EA}(\text{O}) - \gamma(\Omega_{\text{O}^-} - \Omega_X) - mW(1/M_{\text{O}^-} - 1/M_X) \quad (3)$$

oxygen atom which is appropriate for the center of the O^- photodetachment peak at this resolution,¹⁷ and $(\Omega_{\text{O}^-} - \Omega_X)$ is the measured laboratory energy difference between the O^- peak center and a particular electron energy. The factor γ is an energy scale compression factor described previously,¹⁸ for these experiments γ was determined to be 1.0203 by calibrating the spectrum of Cr^{18} with the known value for the $^5\text{S}_2 - ^7\text{S}_3$ energy difference.¹⁹ The final term in eq 3 is a small kinematic correction which results from the fact that the collected electrons are backscattered in the center-of-mass frame; in this term W is the ion beam kinetic energy (680 eV), and m , M_{O^-} , and M_X are the masses of the electron, oxygen atom, and the molecule X, respectively. In general, the electron kinetic energy corresponding to the center of a peak can then be determined to within 0.007 eV. The electron kinetic energy can then be used to determine the electron affinity, $\text{EA}(X)$, as given by eq 4.

$$\text{EA}(X) = h\nu - E_X \quad (4)$$

All data were obtained with the laser polarization oriented at the "magic angle" ($54^\circ 44'$) with respect to the electron collection direction. Thus, the data represent an average photodetachment cross section independent of the angular distribution of the detached electrons.²⁰

For these experiments the $\text{Ni}(\text{CO})_n^-$, $n = 0-3$, ions were produced in an electrical discharge in a 1:1 mixture of $\text{Ni}(\text{CO})_4$ and CO at a total

(1) Tumas, W.; Gitlin, B.; Rosan, A. M.; Yardley, J. T. *J. Am. Chem. Soc.* **1982**, *104*, 55. Nathanson, G.; Gitlin, B.; Rosan, A. M.; Yardley, J. T. *J. Chem. Phys.* **1981**, *74*, 361. Yardley, J. T.; Gitlin, B.; Nathanson, G.; Rosan, A. M. *Ibid.* **1981**, *74*, 370, and references therein.

(2) Vaida, V.; Cooper, N. J.; Hemley, R. J.; Leopold, D. G. *J. Am. Chem. Soc.* **1981**, *103*, 7022. Rothberg, L. J.; Gerrity, D. P.; Vaida, V. *J. Chem. Phys.* **1981**, *74*, 2218, and references therein.

(3) Walch, S. P.; Goddard, W. A., III *J. Am. Chem. Soc.* **1976**, *98*, 7908.

(4) Rives, A. B.; Fenske, R. F. *J. Chem. Phys.* **1981**, *75*, 1293.

(5) Dunlap, B. I.; Yu, H. L.; Antoniewicz, P. R. *Phys. Rev. A* **1982**, *25*, 7.

(6) Bagus, P. S.; Roos, B. O. *J. Chem. Phys.* **1981**, *75*, 5961.

(7) Howard, I. A.; Pratt, G. W.; Johnson, K. H.; Dresselhaus, G. *J. Chem. Phys.* **1981**, *74*, 3415.

(8) Compton, R. N.; Stockdale, J. A. D. *Int. J. Mass Spectrom. Ion Phys.* **1976**, *22*, 47.

(9) Dunbar, R. C.; Hutchinson, B. B. *J. Am. Chem. Soc.* **1974**, *96*, 3816.

(10) Burdett, J. K. *J. Chem. Soc., Chem. Commun.* **1973**, 763.

(11) Breeze, P. A.; Burdett, J. K.; Turner, J. J. *Inorg. Chem.* **1981**, *20*, 3369.

(12) DeKock, R. L. *Inorg. Chem.* **1971**, *10*, 1205.

(13) Burdett, J. K. *Inorg. Chem.* **1975**, *14*, 375.

(14) Elian, M.; Hoffman, R. *Inorg. Chem.* **1975**, *14*, 1058.

(15) Pensak, D. A.; McKinney, R. J. *Inorg. Chem.* **1979**, *18*, 3407. McKinney, R. J.; Pensak, D. A. *Ibid.* **1979**, *18*, 3413.

(16) Celotta, R. J.; Bennett, R. A.; Hall, J. L. *J. Chem. Phys.* **1974**, *60*, 1740. Seigel, M. W.; Celotta, R. J.; Hall, J. L.; Levine, J.; Bennett, R. A. *Phys. Rev. A* **1972**, *6*, 607.

(17) Hotop, H.; Lineberger, W. C. *J. Phys. Chem. Ref. Data* **1975**, *4*, 539. Hotop, H.; Bennett, R. A.; Lineberger, W. C. *J. Chem. Phys.* **1973**, *58*, 2373.

(18) Feigerle, C. S.; Corderman, R. R.; Bobashev, S. V.; Lineberger, W. C. *J. Chem. Phys.* **1981**, *74*, 1580, and references therein.

(19) Moore, C. E. "Atomic Energy Levels", National Bureau of Standards: Washington, DC, 1958; Vol. II.

(20) Cooper, J.; Zare, R. N. *J. Chem. Phys.* **1968**, *48*, 942.

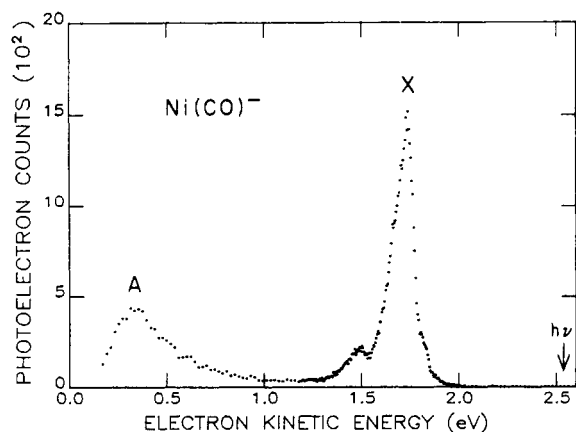


Figure 1. Photoelectron spectrum of $\text{Ni}(\text{CO})_1^-$ obtained with 2.540-eV photons; ion current was about 18 pA. Peak X corresponds to the transition to ground-state $\text{Ni}(\text{CO})$ which defines the electron affinity.

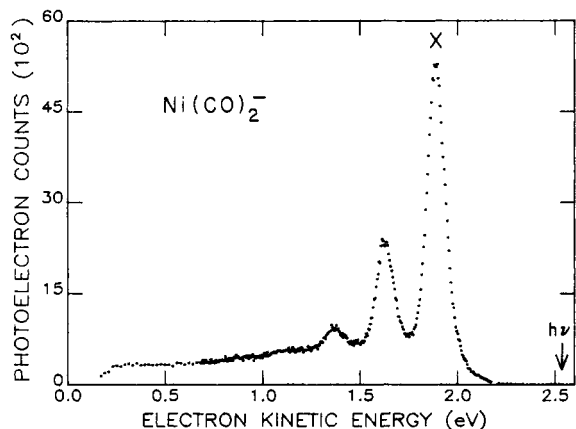


Figure 2. Photoelectron spectrum of $\text{Ni}(\text{CO})_2^-$ obtained with 2.540-eV photons and an ion current of 150 pA. The electron affinity is obtained from peak X.

pressure of about 100 μ . Mass resolution of this instrument is such that the Ni isotopes can be resolved and $^{58}\text{Ni}^-$ and $^{58}\text{Ni}(\text{CO})^-$ clearly identified. For $\text{Ni}(\text{CO})_2^-$ and $\text{Ni}(\text{CO})_3^-$ the two nickel isotopes result in a single broad peak in the ion current.

An approximately 1-kV/cm field is used to extract the ions from the source into a chamber differentially pumped and maintained at $2\text{--}4 \times 10^{-5}$ torr. Collisions between the accelerating ions and the neutral gas occur in the extraction region and result in heating of the negative ions. Previously reported spectra typically show negative ion vibrational populations corresponding to a temperature of 1000 ± 400 K.²¹ An important modification for the present experiment was to change slightly the configuration of the exit aperture from the source to provide much lower pressure in the region of the high extraction field. As such, this source produces vibrationally, and presumably rotationally, cooler ions than had been possible with the previous configuration. By adjustment of source parameters, an O_2^- vibrational temperature of 450 ± 50 K was evident from the spectrum of O_2^- . A more typical temperature is probably 600 ± 200 K.

Because of these changes, we also examined the spectra of $\text{Fe}(\text{CO})_n^-$, $n = 1\text{--}3$, previously obtained on this instrument and reported by Engelking and Lineberger.²² $\text{Fe}(\text{CO})_3$ was dissociated in the discharge source to produce these ions, and several spectra were obtained for each ion at source pressures from 40 to 160 μ .

Results

The spectra of $\text{Ni}(\text{CO})_n^-$, $n = 1\text{--}3$, are given in Figures 1–3. Each of these spectra shows a very sharp peak, labeled X, which we assign to the transition from the vibrationless level of the negative ion to the vibrationless level of the neutral. Additionally,

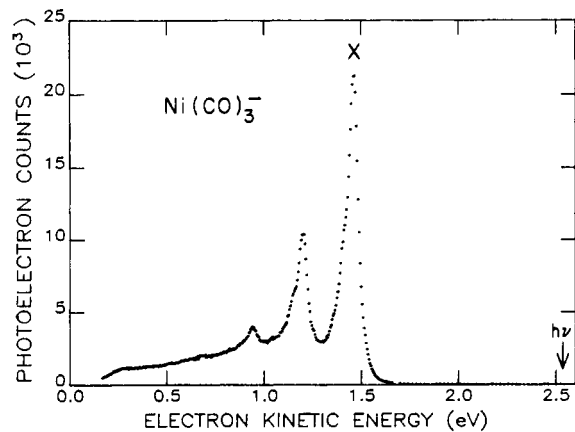


Figure 3. Photoelectron spectrum of $\text{Ni}(\text{CO})_3^-$ obtained with 2.540 eV photons and an ion current of 6.0 nA; the electron affinity is again determined from the peak labeled X.

a vibrational progression at a frequency appropriate for a C–O stretching vibration occurs for each of these molecules. The electron-energy resolution does not allow resolution of rotational structure in these bands, and both inherent energy resolution and rotational broadening obscure Ni–C stretches (typically $400\text{--}600$ cm^{-1}),²³ Ni–C–O bending vibrations (~ 600 cm^{-1}),²³ and C–Ni–C bending vibrations (~ 100 cm^{-1}).²⁴

$\text{Ni}(\text{CO})^-$. The $\text{Ni}(\text{CO})^-$ photoelectron spectrum (Figure 1) shows a strong peak X at 1.734 ± 0.010 eV electron energy, a less intense peak at 1.494 ± 0.010 eV, and a very broad peak A at 0.36 ± 0.02 eV. The decrease in intensity at about 0.25 eV in each spectrum is an artifact which results from the electron-energy analyzer cutoff for very-low-energy electrons; the low-energy feature for $\text{Ni}(\text{CO})^-$ was not examined at higher photon energies which might have indicated further extent of this feature.

Peak X would give $\text{EA}[\text{Ni}(\text{CO})] = 0.806 \pm 0.010$ eV, except that the center of peak X does not determine the electron affinity of $\text{Ni}(\text{CO})^-$. Rather, the peak center corresponds to detachment from the maximally populated rotational level of the ion. This results in a change in rotational energy on detachment which shifts the apparent EA to too high a value. A correction, ΔF , for this is given by eq 5;¹⁶ substituting the rotational constants $B' \sim 0.15$

$$\Delta F = (B' - B'')(kT/2B'' - 1/4) \quad (5)$$

cm^{-1} for $\text{Ni}(\text{CO})$, $B'' \sim 0.14$ cm^{-1} for $\text{Ni}(\text{CO})^-$, and $T \sim 600 \pm 200$ K yields of $\Delta F = 0.002 \pm 0.002$ eV.

Peak X is quite asymmetric; the low-electron-energy side very gradually decreases in intensity. This tail is not smooth, nor is the "peak" itself, both indications of underlying structure. This is often an indication of a vibrational sequence band, which would also shift the center of peak X from the position of the electron-affinity-defining transition. The $\nu(\text{CO})$ are of sufficiently high energy as to be resolved in the spectrum, and no CO excitation in $\text{Ni}(\text{CO})^-$ is seen. The Ni–C–O bending vibration is not expected to be excited since $\text{Ni}(\text{CO})$ and $\text{Ni}(\text{CO})^-$ are both linear. The most likely candidate for a vibrational sequence is thus the low-frequency Ni–C stretching mode. A model of this peak by Franck–Condon analysis of the electron-detachment process was tried. In this model CO is kept fixed and only the Ni–C bond changed. The molecular parameters of Rives and Fenske⁴ were assumed for $^1\Sigma^+\text{Ni}(\text{CO})$; various estimates for ω_c and $\omega_c X_c$ of $\text{Ni}(\text{CO})^-$ were taken (the analysis is relatively insensitive to these). A reasonable fit for peak X was obtained with a change in r_c of about 0.08 Å. The fit is quite insensitive to the temperature, since the vibrations are so closely spaced as to make a relatively smooth peak. The fit indicates that any shift of the peak position by the

(21) Engelking, P. C.; Corderman, R. R.; Wendoloski, J. J.; Ellison, G. B.; O'Neil, S. V.; Lineberger, W. C. *J. Chem. Phys.* **1981**, *74*, 5460, and references therein.

(22) Engelking, P. C.; Lineberger, W. C. *J. Am. Chem. Soc.* **1979**, *101*, 5569.

(23) Nakamoto, K. "Infrared Spectra of Inorganic and Coordination Compounds"; Wiley: New York, 1970. Darenbourg, M. Y.; Darenbourg, D. J. *Inorg. Chem.* **1970**, *9*, 32, and references therein.

(24) Jones, L. H.; McDowell, R. S.; Goldblatt, M.; Swanson, B. I. *J. Chem. Phys.* **1972**, *57*, 2050.

Table I. Electron Affinities, Nickel-Carbonyl Bond Energies, and C-O Vibrational Frequencies for Ni(CO)_n

	EA[Ni(CO) _n], eV	D[Ni(CO) _{n-1} -CO], ^a kcal/mol	$\nu_{01}(\text{C-O}), \text{cm}^{-1}$		
			this work	argon matrix	
				symmetric	antisymmetric
Ni(CO) ₄	<i>c</i>	25 ± 2		2052 ^d	2134
Ni(CO) ₃	1.077 ± 0.013	13 ± 10	2100 ± 80	2016 ^e	2120
Ni(CO) ₂	0.643 ± 0.014	54 ± 15	2100 ± 80	1967 ^f	2090
Ni(CO)	0.804 ± 0.012	29 ± 15	1940 ± 80	1996 ^f	
Ni	1.157 ± 0.010 ^g				

^a Calculated from $D[\text{Ni}(\text{CO})_{n-1}-\text{CO}]$ (Table II) and the electron affinities reported here, as discussed in the text. The very large error limits reported for the $n = 1-3$ cases result almost entirely from the large errors in the appearance potential data given in Table II. ^b Calculated from the Cotton-Kraihanzel force constants given in ref 12. ^c Ni(CO)₄⁻ is not bound with respect to CO dissociation. ^d References 10 and 12. ^e References 10 and 11. ^f Reference 12. ^g Reference 26.

vibrational hot bands is not large with respect to our error limits. Therefore, we neglect any correction to the electron affinity that a vibrational sequence might make, particularly since the correction does depend on the exact vibrational frequencies for ion and neutral.

Peak X also has a shoulder lying about 700 cm⁻¹ to the high-energy side, which does not fit the Franck-Condon analysis of the Ni-C stretch. The frequency suggests this is an excited Ni-C-O bending vibration in the negative ion, but the exact assignment of this peak is uncertain.

The recommended value for EA[Ni(CO)] is thus 0.804 ± 0.012 eV. The peak at 1.494-eV electron energy is assigned to excitation of the C-O stretch of Ni(CO), giving a $\nu_{01}(\text{C-O}) = 1940 \pm 80$ cm⁻¹. The peak at 0.36 eV is clearly an excited electronic state of Ni(CO), which lies 1.37 ± 0.03 eV above the ground state.

Ni(CO)₂⁻. The intense transition for Ni(CO)₂⁻, peak X in Figure 2, occurs at 1.895 ± 0.012 eV electron energy. Similarly to Ni(CO)⁻, a correction of 0.002 ± 0.002 eV is made to account for the change in rotational energy; an adjustment for vibrational sequence bands is not made. A final value EA[Ni(CO)₂] = 0.643 ± 0.014 eV is chosen. Strong transitions at 1.634 ± 0.012 and 1.372 ± 0.012 eV are attributed to the symmetric C-O stretch of Ni(CO)₂, and yield values $\nu_{01}(\text{C-O}) = 2100 \pm 80$ cm⁻¹ and $\nu_{12}(\text{C-O}) = 2120 \pm 80$ cm⁻¹. These peaks all appear much more broadened at the top than is consistent with a single transition; peak positions were chosen as the peak center, but are somewhat more uncertain than for Ni(CO)⁻. Excited C-Ni-C bends of Ni(CO)₂⁻ may contribute to the broadened peak shape. A slight shoulder at about 800 cm⁻¹ to the high-energy side of peak X is tentatively assigned to excited Ni-C-O bending vibrations in Ni(CO)₂⁻. Additionally, the three intense peaks show a great deal of tailing to low electron energy.

Ni(CO)₃⁻. The spectrum of Ni(CO)₃⁻ (Figure 3) is very similar to those of the other two carbonyl ions, with the intense peak X at 1.460 ± 0.010 eV electron energy. While both Ni(CO)₃⁻¹¹ and Ni(CO)₃^{10,12} are trigonal planar (*D*_{3h}), again their exact geometries are not known; a rotational correction of 0.003 eV is estimated. The recommended EA[Ni(CO)₃] is then 1.077 ± 0.013 eV, again neglecting a correction for vibrational sequence bands.

Two strong transitions appear at 1.199 ± 0.010 eV and 0.942 ± 0.010 eV. These are ascribed to the symmetric C-O stretch in Ni(CO)₃, with $\nu_{01}(\text{C-O}) = 2100 \pm 80$ cm⁻¹ and $\nu_{12}(\text{C-O}) = 2075 \pm 80$ cm⁻¹. Again, each of these peaks shows strong tailing to low-electron energies.

The intense peaks X of each ion, as well as the low-electron-energy peak A of Ni(CO)⁻ were studied as a function of laser power. Count rates in all cases are found to be first order in laser power, indicating the spectra result from single-photon processes. The count rates can also be used to establish the total relative cross sections for electron detachment; these are 34:8:2:3:6 for Ni⁻/Ni(CO)⁻/Ni(CO)₂⁻/Ni(CO)₃⁻/O⁻. The count rate for O⁻ is given as a reference; it has a total cross section for electron detachment of about 6 × 10⁻¹⁸ cm².²⁵ The relative values are accurate to a factor of 2.

Table II. Appearance Potentials of Ni(CO)_n⁻ from Ni(CO)₄ and Carbonyl Bond Energies for the Ni(CO)_n⁻ Ions

	AP[Ni(CO) _n ⁻], ^a eV	D[Ni(CO) _{n-1} -CO], kcal/mol
Ni(CO) ₄ ⁻	<i>b</i>	
Ni(CO) ₃ ⁻	0.0	23 ± 9
Ni(CO) ₂ ⁻	1.0 ± 0.4	51 ± 15
Ni(CO) ⁻	3.2 ± 0.5	21 ± 15
Ni ⁻	4.1 ± 0.3	
	4.96 ± 0.12 ^c	

^a All appearance potentials are taken from the figures of ref 8; an exception is AP[Ni⁻], which value Compton and Stockdale chose. ^b Ni(CO)₄⁻ is not bound with respect to dissociation of CO. ^c Predicted AP[Ni⁻] based upon EA[Ni] = 1.157 ± 0.012 eV²⁶ and $\bar{D}[\text{Ni-CO}] = 1.53 \pm 0.03$ eV,²⁷ as discussed in the text.

Discussion

The electron affinities of the nickel carbonyls, and the electron affinity of nickel which was determined by these methods and previously reported,²⁶ are summarized in Table I. The individual bond energies, $D[\text{Ni}(\text{CO})_{n-1}-\text{CO}]$ of the neutral molecules, $n = 1-3$, are calculated as shown in Figure 4 and eq 6 using Ni(CO)

$$D[\text{Ni-CO}] = D[\text{Ni}^--\text{CO}] + \text{EA}[\text{Ni}] - \text{EA}[\text{Ni}(\text{CO})] \quad (6)$$

as an example. All bond energies for the negative ions are taken from the appearance potential data of Compton and Stockdale,⁸ these are summarized in Table II. $D[\text{Ni}(\text{CO})_3-\text{CO}]$ is determined by the thermoneutrality of reaction 1 for $n = 3$;⁸ that is, $D[\text{Ni}(\text{CO})_3-\text{CO}] \approx \text{EA}[\text{Ni}(\text{CO})_3]$. An average bond energy, $\bar{D}[\text{Ni-CO}] = 30 \pm 3$ kcal/mol for all four carbonyls is calculated from EA[Ni] = 1.157 ± 0.010 eV²⁶ and AP[Ni⁻] = 4.1 ± 0.3 eV (chosen by Compton and Stockton⁸) (Tables I and II). This value is somewhat lower than the accepted value, $\bar{D}[\text{Ni-CO}] = 35.3 \pm 0.6$ kcal/mol.²⁷ In fact, this average bond energy and EA[Ni] would predict the AP[Ni⁻] to be 4.96 ± 0.12 eV, which is a large discrepancy from the value of Compton and Stockdale. The Ni⁻ is only a minor fragment in the negative ion mass spectrum of Ni(CO)₄, with a maximum relative intensity about 1/5000 that of Ni(CO)₃⁻ at its peak. Ni(CO)⁻ is also of quite low intensity. It seems likely that AP[Ni(CO)⁻] should be revised upward as well, probably by about 0.5 eV. These new AP would result in stronger $D[\text{Ni}^--(\text{CO})]$ and $D[\text{Ni}(\text{CO})^--(\text{CO})]$ by about 10 kcal/mol, thus stronger bonds for the corresponding neutrals as well. To be consistent, we report the bond energies derived from the AP's of Compton and Stockdale. Although these are somewhat low bond energies, this in no way affects the conclusions about the electronic and geometric factors which influence the bonding in these complexes.

The vibrational frequency $\nu_{01}(\text{C-O})$ obtained from the PES and the $\nu_{01}(\text{C-O})$ observed in an argon matrix for Ni(CO)_n are compared in Table I. It should be noted that the electron detachment process activates only the totally symmetric C-O stretching mode,²⁸ whereas the IR-active modes correspond to the antisym-

(26) Corderman, R. R.; Engelking, P. C.; Lineberger, W. C. *J. Chem. Phys.* 1979, 70, 4474.

(27) Distefano, G. *J. Res. Natl. Bur. Stand., Sect. A* 1970, 74, 233, and references therein.

(25) Branscomb, L. M.; Smith, S. J.; Tison, G. *J. Chem. Phys.* 1965, 43, 2906.

metric stretch. For monocarbonyl, of course, such a distinction does not exist. The symmetric $\nu_{01}(\text{CO})$ for the matrix-isolated $\text{Ni}(\text{CO})_n$ can be obtained from the Cotton-Kraihanzel force constants;¹² these values are also reported in Table I for comparison.

The spectra and associated thermodynamics for the nickel carbonyls are extremely surprising in several ways. First, the EA's of the $\text{Ni}(\text{CO})_n$ are decidedly *not* linear with n ; rather, they *decrease* from $n = 0$ to $n = 1$ and 2, and even $\text{Ni}(\text{CO})_3$ does not attain as high an electron affinity as the Ni atom. Second, the individual bond energies are very disparate from $\bar{D}[\text{Ni}-\text{Co}]$, with a maximum of $D[\text{Ni}(\text{CO})-\text{CO}] = 54$ kcal/mol and $D[\text{Ni}(\text{CO})_2-\text{CO}]$ a mere 13 kcal/mol. Third, it is remarkable that these spectra show vibrational structure at all; the photoelectron spectra of neutral carbonyls show virtually none,²⁹ and even the $\text{Fe}(\text{CO})_n^-$ spectra are quite broad and featureless.²² To understand this behavior, we treat each molecule separately to find the electronic and geometric factors which determine the molecular properties.

Structure of $\text{Ni}(\text{CO})_n$ and $\text{Ni}(\text{CO})_n^-$. $\text{Ni}(\text{CO})_4$ is a closed-shell 18-electron tetrahedral complex, in which the Ni may be thought of as in a d^{10} -like configuration. No data are available on its electron affinity, since the attachment of a zero-energy electron results in $\text{Ni}(\text{CO})_3^-$ production by an approximately thermoneutral process.⁸

Observation of the ^{12}CO and ^{13}CO stretching frequencies has identified matrix-isolated $\text{Ni}(\text{CO})_3^-$ as having a trigonal planar (D_{3h}) geometry, since only the single antisymmetric stretching mode is observed.^{10,11} The corresponding neutral, $\text{Ni}(\text{CO})_3$, is similarly identified by its IR spectrum; it, too, is of trigonal planar geometry.¹² A shift of 158 cm^{-1} is seen between $\nu_{01}(\text{CO}) = 2016\text{ cm}^{-1}$ in $\text{Ni}(\text{CO})_3$ and $\nu_{01}(\text{CO}) = 1858\text{ cm}^{-1}$ of the anion. Although this is the expected direction of change, it is significantly greater than the $110\text{--}124\text{ cm}^{-1}$ observed¹¹ between five other neutral carbonyls and their corresponding anions. This is taken as evidence that the "extra electron" of the anion does not enter the d shell.¹¹ The photodecomposition of $\text{Ni}(\text{CO})_3^-$ reported from the ICR experiments is also anomalous.⁹ The peak at 2.5 eV in the "photodisappearance" spectrum was ascribed to an optical absorption of the $\text{Ni}(\text{CO})_3^-$, shifted higher in energy than expected by comparison with $\text{Cr}(\text{CO})_3^-$ and $\text{Co}(\text{CO})_3^-$. This shift was attributed to $\text{Ni}(\text{CO})_3^-$ being of s^1d^{10} configuration, while the other tricarbonyl negative ions are of d^n configuration.⁹ These pieces of evidence, as well as several semiempirical molecular orbital calculations on $\text{Ni}(\text{CO})_3$,^{7,13-15} lead to establishment of $\text{Ni}(\text{CO})_3$ as a d^{10} , trigonal-planar molecule, and $\text{Ni}(\text{CO})_3^-$ having an s^1d^{10} configuration and like geometry.

Although observed in mass spectra,⁸ $\text{Ni}(\text{CO})_2^-$ has not been identified in other experiments. The antisymmetric $\nu(\text{CO}) = 1967\text{ cm}^{-1}$ of $\text{Ni}(\text{CO})_2$ isolated in an argon matrix has been used to identify the molecule as having a linear geometry.¹² Molecular orbital calculations suggest it has a d^{10} configuration,^{7,13} but detailed calculations or experimental evidence for this do not exist. We expect $\text{Ni}(\text{CO})_2^-$ to be linear as well, with an s^1d^{10} configuration.

$\text{Ni}(\text{CO})^-$ is observed in the negative ion mass spectrum, but again has not been detected using other techniques. Although Ni^- has a configuration s^2d^9 ,²⁶ CO is not expected to bind to this state, because of repulsion between the σ -donor electrons of CO and the s^2 electrons of Ni^- . Rather, it is again expected that $\text{Ni}(\text{CO})^-$ has an s^1d^{10} configuration, which yields a $^2\Sigma^+$ ground state. Although a $\nu(\text{CO}) = 1996\text{ cm}^{-1}$ is reported for matrix-isolated $\text{Ni}(\text{CO})$,¹² and it is expected to be linear, its electronic structure is not firmly established. Possible electronic states include the $^1\Sigma^+$, derived principally from a d^{10} Ni, or the $^3\Delta$, $^3\Sigma^+$, and $^3\Pi$ states which result from bonding the CO to an s^1d^9 nickel atom. All of these states are accessible by one-electron transitions from

$s^1d^{10}\text{ Ni}(\text{CO})^-$, either by loss of the s electron, to give the $^1\Sigma^+$ state, or loss of a d electron to give the $^3\Delta$, $^3\Sigma^+$, or $^3\Pi$ states of $\text{Ni}(\text{CO})$.

Whereas it is difficult to establish unequivocally the electronic configuration based upon the photoelectron spectrum, the spectrum of $\text{Ni}(\text{CO})^-$ is consistent with the theoretical predictions of Rives and Fenske⁴ and Dunlap, Yu, and Antoniewicz⁵ of a $\text{Ni}(\text{CO})$ ground state $^1\Sigma^+$. In particular, the spectrum shows two electronic states, with a 1.37-eV excitation to the upper state, in agreement with the calculated 1.2⁴ or 1.8 eV⁵ excitation to the $^3\Delta$ state. Transitions to the $^3\Delta$, $^3\Sigma^+$, and $^3\Pi$ states may all contribute to peak A. State A is about 3 ± 15 kcal/mol above the calculated dissociation limit to yield $\text{Ni}(s^2d^8)$ and CO, or very nearly thermoneutral for dissociation to either ground-state products or $\text{Ni}(s^1d^9)$ which is of comparable energy.¹⁹ The broad peak observed may be an indication of the weakly bound character of this state, again in agreement with the predictions for the triplet states.^{4,5} Finally, the $\text{Ni}(\text{CO})^-$ electron-detachment cross section to peak X is comparable to the total electron-detachment cross sections of $\text{Ni}(\text{CO})_2^-$ and $\text{Ni}(\text{CO})_3^-$, which are both s-electron detachments. For the metal atoms, s-electron detachments are of much greater intensity than d-electron detachments.¹⁸ This observation is consistent with peak X being an s-electron and peak A being a d-electron detachment.

Somewhat unexpected is the Franck-Condon analysis of the $\text{Ni}(\text{CO})^-$ spectrum, which indicates a change of 0.08 \AA in $r_e(\text{Ni}-\text{C})$ on electron detachment to state X. This seems consistent only with a nonbonding (d electron) detachment, with the s electron in both ion and neutral causing a fairly long $r_e(\text{Ni}-\text{C})$. The triplet states of $\text{Ni}(\text{CO})$ are predicted to have an $r_e(\text{Ni}-\text{C})$ of about 0.25 \AA longer than in the $^1\Sigma^+$ state;³⁻⁵ the antibonding s electron of $\text{Ni}(\text{CO})^-$ might be expected to have a similar effect on the bond length. Using a $\Delta r_e = 0.25\text{--}0.3\text{ \AA}$ in the Franck-Condon analysis yields a peak envelope strongly skewed to low-electron energies, and twice as broad as the observed peak X.

However, it is not clear that the expectations for a long $r_e(\text{Ni}-\text{C})$ of $\text{Ni}(\text{CO})^-$ are realistic. In the case of $\text{Ni}(\text{CO})_2^-$ and $\text{Ni}(\text{CO})_3^-$, the observed spectra are interpreted as arising from s-electron detachment, but in these spectra the peaks are of comparable shape as peak X of $\text{Ni}(\text{CO})^-$. It appears that the added s electron in each of the three negative ions is strongly delocalized (π -back-bonding) onto the CO ligands. Thus, the Ni-C bond stays about the same length, with the $r_e(\text{C}-\text{O})$ increasing "substantially" in the negative ion. The "s"-electron detachment results in the observed vibrational progression in the C-O stretch, but not an extended progression in the Ni-C stretching mode. We can now reexamine the trends in the electron affinities and bond energies for the carbonyl series.

Examination of the $\text{Ni}(\text{CO})_n$ Molecular Properties. First, the electron affinities of the carbonyls are all determined by a $d^{10} \leftarrow s^1d^{10}$ transition, while for the nickel atom, the electron affinity corresponds to an $s^2d^8 \leftarrow s^2d^9$ transition.²⁶ Thus, for a direct comparison between the electron affinities of the nickel atom and the carbonyl complexes, the energy of the $\text{Ni } d^{10} \leftarrow \text{Ni}^- s^1d^{10}$ transition is needed. The s^1d^{10} state of Ni^- has not been observed, and it is likely that it is not bound with respect to $\text{Ni} + e$. The decrease in the electron affinities of the carbonyl complexes with respect to that of the nickel atom is in part a reflection of this change in electronic configuration. Another influence in determining the electron affinities of the carbonyls is, of course, the CO. The nickel s electron in $\text{Ni}(\text{CO})^-$ is antibonding with respect to the Ni-C σ bond. This antibonding character will cause the "s" electron to mix in Ni p- σ character, resulting in a shift of the electron density to the backside of the Ni, away from the Ni-C bond.³ The "s"-electron antibonding character is evidenced by a decrease in electron affinity from $\text{Ni}(\text{CO})$ to $\text{Ni}(\text{CO})_2$; the ability of the "s" electron to move away from the Ni-C σ bonds is lost when the second CO binds. The extended progressions in the C-O stretching vibration in the spectra of $\text{Ni}(\text{CO})_2^-$ and $\text{Ni}(\text{CO})_3^-$, as well as the increase in electron affinity from $\text{Ni}(\text{CO})_2$ to $\text{Ni}(\text{CO})_3$, provide evidence that the "extra" electron in $\text{Ni}(\text{CO})_2^-$ and $\text{Ni}(\text{CO})_3^-$ is substantially delocalized into the π system of the carbonyls. Since the s electron is of the wrong symmetry to

(28) Novick, S. E.; Engelking, P. C.; Jones, P. L.; Futrell, J. H.; Lineberger, W. C. *J. Chem. Phys.* **1979**, *70*, 2652.

(29) Cowley, A. H. "U.V. Photoelectron Spectroscopy in Transition Metal Chemistry". In Lippard, S. J., Ed.; "Progress in Inorganic Chemistry"; Wiley: New York, 1979; Vol. 26 and references therein.

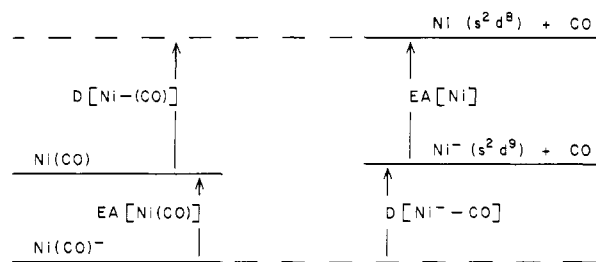


Figure 4. Illustration of the energetic relationship between the negative ion $\text{Ni}(\text{CO})_n^-$ and neutral $\text{Ni}(\text{CO})_n$, from which eq 6 is derived.

do this, there is a possibility that the extra electron is added as a nickel p electron in $\text{Ni}(\text{CO})_2^-$ and $\text{Ni}(\text{CO})_3^-$. There is no information on how high in energy the p^1d^{10} configuration of Ni^- might be, nor are there any calculations on the carbonyl negative ions might help clarify this issue.

The second interesting property is that the Ni-CO bond energies vary so enormously. The $D[\text{Ni}-(\text{CO})]$ from this work may be too low a value, as discussed, because of problems in the appearance potential data. It is a combination of a substantial (1.7 eV¹⁹) excitation of s^2d^8 Ni to the bonding state, d^{10} , but a strong bond (experimentally, 68 kcal/mol) to this state, resulting in a moderate $D[\text{Ni}-(\text{CO})] = 29$ kcal/mol. The very strong $D[\text{Ni}(\text{CO})-\text{CO}] = 54$ kcal/mol fits this analysis; the $1^2\Sigma^+$ state of $\text{Ni}(\text{CO})$ requires no electronic excitation or geometry change to bind the second CO. Why $D[\text{Ni}(\text{CO})_2-\text{CO}] = 13$ kcal/mol is so weak is not clear. No electronic excitation is required, and although a bending of the carbonyls from 180° to 120° with respect to each other occurs, it does not seem it should be so costly energetically. Ligand-ligand repulsion could play a role. Finally, $D[\text{Ni}(\text{CO})_3-\text{CO}] = 25$ kcal/mol is of moderate strength. Addition of CO to the trigonal planar $\text{Ni}(\text{CO})_3$ requires less geometry change, with the C-Ni-C angle going from 120° to the 109° of a tetrahedral molecule. This value agrees very well with a $\Delta H_{\text{activation}}$ of about 22 kcal/mol for the gas-phase decomposition of $\text{Ni}(\text{CO})_4$.³⁰ The activation energy was attributed to loss of CO, but this could not be proven.

From Table I, it can be seen that the $\nu_{01}(\text{CO})$ increase quite regularly with increasing coordination number. This increase in $\nu(\text{CO})$ is often taken as an indication of a decrease in $D[\text{Ni}(\text{CO})_n-\text{CO}]$ with increasing n . The $\nu_{01}(\text{CO})$, however, really reflect the vibrational frequency at the bottom of the $\text{Ni}(\text{CO})_n-\text{CO}$ bonding potential well. Thus, the CO frequency changes are expected to be better correlated with the bond energies of CO to a $\text{Ni}(\text{CO})_n^*$ with the proper geometry and electronic state appropriate for bonding the $(n+1)$ th CO, than the $D[\text{Ni}(\text{CO})_n-\text{CO}]$. As an example, the $\nu_{01}(\text{CO})$ for $\text{Ni}(\text{CO})$ is a low 1996 cm^{-1} . This is a reflection of the strong CO bond of 68 kcal/mol to the excited $\text{Ni}(d^{10})$, which is quite different from the much weaker 29 kcal/mol of the thermodynamic bond energy. Similar considerations might be expected to hold for the other species.

Finally, the reason for the relatively sharp peaks and well-resolved CO vibrational progressions in the photoelectron spectra is now clear. The ground state of each of the $\text{Ni}(\text{CO})_n$ is a totally symmetric singlet state; the $\text{Ni}(\text{CO})_n^-$ are totally symmetric doublets. Thus, the electronic structure dictates a single transition. Second, although $r_e(\text{Ni}-\text{C})$ and $r_e(\text{C}-\text{O})$ clearly change on loss of the electron, in no instance does the C-Ni-C angle change. Carbon-metal-carbon bending modes are typically about 100 cm^{-1} .²⁴ Not only would the enormous vibrational progression of the neutral be unresolvable at our resolution if this mode were excited, but at our source temperatures (~ 600 K), the hot-band structure would further obscure the transitions, resulting in broad, featureless spectra.

Comparison to the $\text{Fe}(\text{CO})_n^-$ Spectra. The only data available for direct comparison are from the $\text{Fe}(\text{CO})_n^-$, $n = 1-4$, ions. By contrast, the electron affinities for the $\text{Fe}(\text{CO})_n$ increase roughly

linearly with n ,²² although the parent ion, $\text{Fe}(\text{CO})_5^-$, is again not bound with respect to loss of CO.⁸ The individual bond energies are rather varied, with a strong $D[\text{Fe}(\text{CO})_4-\text{CO}] = 48 \pm 4$ kcal/mol,³¹ and $D[\text{Fe}(\text{CO})_3-\text{CO}] = 5 \pm 7$ kcal/mol²² the weakest bond.

But quite differently, the $\text{Fe}(\text{CO})_n^-$ ions show extremely broadened, featureless spectra, with only $\text{Fe}(\text{CO})^-$ and $\text{Fe}(\text{CO})_2^-$ exhibiting peaks attributable to a CO vibrational progression. Because of the source modifications mentioned, we repeated the work for $\text{Fe}(\text{CO})^-$, $\text{Fe}(\text{CO})_2^-$, and $\text{Fe}(\text{CO})_3^-$; essentially the same spectra were obtained. The only notable exception was that the electron-affinity-defining peak in $\text{Fe}(\text{CO})^-$ was much better resolved and showed three maxima, due both to better electron-energy resolution and probably a colder ion. In fact, in the published spectrum it exhibits an oddly shaped peak which hints at underlying structure.

Interestingly, both $\text{Fe}(\text{CO})_2^-$ and $\text{Fe}(\text{CO})_3^-$ were originally reported²² to have features to the right of the electron-affinity-defining peak. In the spectrum of $\text{Fe}(\text{CO})_2^-$ this was tentatively assigned as the C-O stretch of $\text{Fe}(\text{CO})_2^-$, although it was noted this gave a high value, 2250 ± 100 cm^{-1} , inconsistent with the decrease in $\nu(\text{CO})$ expected from π -back-bonding considerations. The peak at about 4000 cm^{-1} in the tricarbonyl was suggested to be a transition from an excited electronic state of $\text{Fe}(\text{CO})_3^-$.

We have reexamined the photoelectron spectra of the $\text{Fe}(\text{CO})_2^-$ and $\text{Fe}(\text{CO})_3^-$ ions at several ion source pressures, in an attempt to identify these spectral features. At the higher source pressures, the small peaks observed in the $\text{Fe}(\text{CO})_2^-$ and $\text{Fe}(\text{CO})_3^-$ spectra increase from about 10 to 40% of the intensity of the strongest transition, inconsistent with their being transitions from excited states of those ions. At these higher pressures as well, substantial currents of $\text{Fe}_2(\text{CO})_n^-$, $n \geq 3$, are readily produced. We now attribute the small peak seen in the $\text{Fe}(\text{CO})_2^-$ spectrum²² to the Fe_2^- ion (both these ions have $m/e = 112$) and that in the $\text{Fe}(\text{CO})_3^-$ spectrum²² to $\text{Fe}_2(\text{CO})^-$ ($m/e = 140$) which are apparently formed by ion clustering.

The spectra of the iron carbonyls result from geometry changes which excite the C-Fe-C low-frequency bending vibrations, as well as broadening by multiplet states of ion and neutral. They thus confirm our assignment of the simplicity of the electron-detachment processes for the nickel carbonyl ions.

Conclusions

The photoelectron spectra of the nickel carbonyl ions can be used to directly determine $EA[\text{Ni}(\text{CO})] = 0.804 \pm 0.012$ eV, $EA[\text{Ni}(\text{CO})_2] = 0.643 \pm 0.014$ eV, and $EA[\text{Ni}(\text{CO})_3] = 1.077 \pm 0.013$ eV. Each of the spectra exhibit clearly resolved progressions in the C-O symmetric stretching vibration of the corresponding neutral carbonyl. The electron affinities are used in conjunction with appearance potential data to establish the individual bond energies of each of the fragments, $D[\text{Ni}(\text{CO})_{n-1}-\text{CO}]$, $n = 0-3$. An s^1d^{10} configuration of the $\text{Ni}(\text{CO})_n^-$, and a d^{10} configuration of the $\text{Ni}(\text{CO})_n$ readily explain the observed variation in the electron affinities and the bond energies. Loss of the s electron for the nickel carbonyls is unique in that the spectra are the result of electron detachment from doublet totally symmetric negative ions to give singlet totally symmetric $\text{Ni}(\text{CO})_n$; thus they contain only a single electronic transition in the region of the ground state $\text{Ni}(\text{CO})_n$. Delocalization of the added s electron in $\text{Ni}(\text{CO})_n^-$ results in a fairly small $r_e(\text{Ni}-\text{C})$ change, but appears to increase the C-O distance so as to cause a distinct C-O vibrational progression in the neutral. Finally, the low-frequency C-Ni-C bending modes are not excited by the electron-detachment process, since both ion and neutral in each case are of like geometry, with the C-Ni-C angles remaining the same.

Acknowledgment. This work was supported by Grants PHY79-04928 and CHE78-18424 from the National Science Foundation. A.E.S. gratefully acknowledges support from a

(30) Day, J. P.; Basolo, F.; Pearson, R. G. *J. Am. Chem. Soc.* **1968**, *90*, 6927. Day, J. P.; Pearson, R. G.; Basolo, F. *Ibid.* **1968**, *90*, 693.

(31) Smith, G. P.; Laine, R. M. *J. Phys. Chem.* **1981**, *85*, 1620.

National Science Foundation Postdoctoral Fellowship (1980-1981). W.C.L. was supported by a University of Colorado Faculty Fellowship and a J. S. Guggenheim Foundation Fellowship (1981-1982). We thank H. Benton Ellis, Jr., and G. Barney Ellison for the many discussions which led to the source modi-

fications discussed in this paper.

Registry No. Ni(CO)₂⁻, 82639-17-6; Ni(CO)₂⁻, 82639-18-7; Ni(CO)₃⁻, 51222-94-7; Ni(CO)₄, 13463-39-3; Ni(CO), 33637-76-2; Ni(CO)₂, 33637-77-3; Ni(CO)₃, 26024-55-5.

Observation of Some Transition Metal Complexes in Solution by Electrohydrodynamic Ionization Mass Spectrometry

Kelvin W. S. Chan and Kelsey D. Cook*

Contribution from the School of Chemical Sciences and Materials Research Laboratory, Department of Chemistry, Roger Adams Laboratory, University of Illinois, Urbana, Illinois 61801. Received December 28, 1981

Abstract: Direct mass spectral sampling of glycerol solutions of bipyridyl complexes of ruthenium and chromium has been achieved by electrohydrodynamic ionization. The spectra show no evidence of fragmentation, but do reflect the solution chemistry of the complexes. The ruthenium(II) complex (Ru(bpy)₃²⁺) was stable and inert in solution, whereas the chromium(II) complex (Cr(bpy)₃²⁺) underwent both ligand exchange (with Cl⁻ and glycerol (G)) and oxidation to form a mixture of singly and doubly charged complexes (Cr(bpy)₃²⁺, Cr(bpy)₂Cl⁺, Cr(bpy)₂Cl₂⁺, Cr(bpy)₂(G-2H)⁺, and Cr(bpy)₂Cl(G-H)⁺). Zn(bpy)₂Cl⁺ was detected as impurity in the chromium sample. These results suggest that electrohydrodynamic ionization mass spectrometry should be a valuable probe of the solution chemistry of ion-ligand interactions.

Introduction

An important characteristic of the chemistry of transition metal complexes in solution is their ability to exchange ligands with surrounding species, including solvent molecules. The extent of ligand exchange depends on the thermodynamic stability and kinetic lability of the complex, the ligands involved, and the solvent. While the structure and composition of a complex in the solid state may be characterized by a variety of techniques, these properties may change substantially upon dissolution. It is important to know what species actually exist in solution in order to understand the chemistry of the system.

Solution systems are usually characterized by methods such as electron spin resonance, nuclear magnetic resonance, Raman, infrared, and ultraviolet-visible spectroscopy. These spectroscopic techniques relate the energy of various transitions to the structure of the complex. Generally, two or more of these techniques are used complementarily in the characterization process. Nevertheless, the utility of these approaches is somewhat limited for solutions comprised of a mixture of similar species (or species involved in exchange equilibria) whose spectra may not be resolved, but rather represent the average bulk behavior of the mixture.

Many complexes of similar structure (and therefore similar optical spectroscopy) have appreciably different masses. However, despite the broad utility of mass spectrometry for determination of molecular weights and structures, this information cannot be simply obtained for solution systems by conventional mass spectrometric techniques. These techniques sample molecules from gaseous or solid phase with subsequent or concurrent ionization. For example, the application of standard electron impact mass spectrometry (EIMS)¹ to the analysis of thermally labile, non-volatile samples (such as transition metal complexes) is limited because a large amount of energy is imparted to sample molecules during volatilization and EI ionization. This can grossly affect equilibria and also cause significant fragmentation of molecular ions, often resulting in the loss of molecular weight information. Thus, although the mass spectra obtained from EIMS are often useful for structure determination of analytes, their complexity

impedes application to mixture analysis.

Simpler spectra can be obtained using "soft" ionization processes, which promote less fragmentation. Chemical ionization (CI),² field ionization (FI),³ and field desorption (FD)⁴ are principal examples. In CI and FI, gaseous analytes are ionized by a reagent gas (CI) or an electric field (FI). Solids and liquids must be heated to vaporize as in EI, reducing the applicability of CI and FI for analysis of thermally labile, nonvolatile samples. As a result, FD is often the ionization process of choice for mass spectrometric analysis of nonvolatiles. In a FD ion source, analyte solution is loaded onto an emitter wire. The solvent is subsequently removed by evaporation. Desorption and ionization are promoted by the application of a high electric field between the emitter and extractor. Unfortunately, it is usually necessary to heat the emitter to several hundred degrees, promoting degradation or decomposition of thermally labile nonvolatile samples. Again, resulting fragment ions complicate direct mixture analysis. Furthermore, as for CI and EI, solvent removal precedes FD ionization and may perturb solution equilibria among species to be characterized.

Another family of soft ionization techniques relies on the inefficiency of energy transfer to internal degrees of freedom upon sample bombardment by energetic photons (laser desorption, LDMS),⁵ ions (secondary ion, SIMS),⁶ fission fragments (plasma desorption, PDMS),⁷ or neutral atoms (fast atom bombardment, FABMS).⁸ Of these, all but FABMS have been used primarily for solid samples. For reasons still unclear, FAB ionization is facilitated if the sample is introduced as a glycerol slurry or solution. Thus, of all conventional "soft" ionization methods, FABMS offers the best chance for characterization of solutions. However, appreciable fragmentation always accompanies FAB ionization, which limits applicability for direct mixture analysis.

(2) Munson, B. *Anal. Chem.* **1971**, *43*, 28A-43A.

(3) Beeky, H. D. "Field Ionization Mass Spectrometry"; Pergamon Press: New York, 1971.

(4) Reynolds, W. D. *Anal. Chem.* **1979**, *51*, 283A-293A.

(5) Hercules, D. M.; Day, R. J.; Balasanmugam, K.; Dang, T. A.; Li, C. P. *Anal. Chem.* **1982**, *54*, 280A-305A.

(6) Cooks, R. G.; Day, R. J.; Unger, S. E. *Anal. Chem.* **1980**, *52*, 557A-572A.

(7) Macfarlane, R. D.; Torgerson, D. F. *Science* **1976**, *191*, 920-925.

(8) Barber, M.; Bordoli, R. S.; Elliott, G. J.; Sedgwick, R. D.; Tyler, A. N. *Anal. Chem.* **1982**, *54*, 645A-657A.

(1) Roboz, J. "Introduction to Mass Spectrometry, Instrumentation and Techniques"; Interscience: New York, 1968; Chapter 4.